Eng. & Tech. Journal, Vol.31, No.1, 2013

Experimental Study of Heat Transfer Coefficients of Shell and Helically Coiled Tube Heat Exchangers

Dr. Sattar Jaber Habeeb Al-Jabair
Mechain Engineering Department, University of Technology/Baghdad
Email: hdrsattar@yahoo.com
Ammar.A.Hussain.A.AL-taee
Mechain Engineering Department, University of Technology/Baghdad

Received on: 8/1/2012 & Accepted on: 7/6/2012

ABSTRACT

This work presents an experimental study of the heat transfer coefficients of shell and helically coiled tube heat exchangers. Three heat exchangers with different coil pitches were tested for both parallel-flow and counter-flow arrangement. Water is used as working fluids in shell side and tube side. The study is conducted at the hot water mass flow rates ranging between (0.02 - 0.12) kg/s while cold water is kept constant at (0.055 kg/s). The range of inlet temperatures of cold and hot water are (19 - 28 °C), and (50 - 80 °C), respectively. All experiments were performed at the Dean Number for coiled side range of (3803 - 12117). The work is performed to evaluate the influence of the tube diameter, coil pitch, shell-side and tube-side mass flow rate, and inlet temperatures of tube-side over the axial temperature distribution of heat exchanger, effectiveness, modified effectiveness and heat transfer coefficient. The evaluating has been performed for the steady-state . The results indicate that the major effect on the axial temperature distribution of heat exchanger was the mass flow rate ratio (m_r). Also the modified effectiveness decreased with increasing mass flow rate ratio. The main influence on the shell-side heat transfer coefficient was coil pitch. Develop an equation to correlate Nusselt Number as function of Reynolds Number, Prandtl Number, Dean Number and helical coil Number.

Keywords: Shell and Coiled Tube, Heat Exchanger, Heat Transfer Coefficient.

دراسة عملية لمعامل انتقال الحرارة لمبادل حراري مكون من ملف حلزوني واسطوانة

الخلاصـــــة

يقدم هذا العمل دراسة عملية لمعاملات انتقال الحرارة بالحمل القسري لمبادل حراري مكون من اسطوانة (الصدفة) وانبوب ملفوف بشكل حلزوني. تم اختيار ثلاث ملفات وبدرجات حلزون مختلفة (coil pitches) لمقطع الأختبار وللجريان المتوازي والمتعاكس. تم استعمال الماء البارد والحار كسوائل تشغيل من جانب الأسطوانة والملف الحلزوني على التوالي. جرت الدراسة بنسب

https://doi.org/10.30684/etj.2013.71256
2412-0758/University of Technology-Iraq, Baghdad, Iraq

تدفق للماء الحار تتراوح بين (0.02 - 0.12 kg/s) بينما الماء البارد يبقى ثابت عند 0.055).
(kg/sان مدى درجات الحرارة لدخول الماء البارد والحارتتراوح بين (19 - 28 °C) و(50 - 80 °C) على التوالي. كل التجارب اديت للأعداد دين تتروح بين (12117 - 3803). ان الغرض من هذا العمل هو تقييم تأثير كل من قطر الانبوب ، درجة الحلزون (coil pitches) ومعدل التدفق من جانب الملف ومن جانب الصدفة ودرجة حرارة الدخول من جانب الملف على كل من شكل توزيع درجات الحرارة المحورية داخل المبادل، الفعالية،الفعالية المُعَدلّة ومعامل انتقال الحرارة لكل من الجريان المتوازي والمتعاكس. اخذت جميع القراءات للحالة المستقرة فقط. تشير النتائج أن التأثير الرئيسي على شكل توزيع درجات الحرارة المحورية داخل المبادل الحراري كانت نسبة التدفق (m_r). تشير النتائج ايضاً ان الفعالية المعدلة تقل مع زيادة نسبة التدفق (m_r) . التأثير الرئيسي على معامل انتقال الحرارة الخارجي (h_o) كان درجة الحلزون (coil pitches) . تطوير معادلات لربط عدد نسلت بعدد رينولد وعدد برانتل وعدد دين.

Nomenclature

A	*Area*, m^2	UA	*Overall conductance of heat exchanger, W/°C*
A_c	*surface of the coiled tube*, m^2	U	*Overall heat transfer coefficient, $W/m^2 \cdot K$*
C_r	*Heat capacity ratio of the two fluids (C_{min}/C_{max})*	V	*Velocity, m/s*
Cp	*Specific heat*, *J/kg. K*		***Greek Symbols***
D, d	*Diameter*, m	A	*Thermal diffusivity, m^2/s*
D_h	*Heat exchanger hydraulic diameter* ,m	ΔT	*Temperature difference,* °C
De	*Dean number*	μ	*Fluid viscosity*, *kg/m.s*
H	*Heat exchanger height, m*	P	*Mass density, kg/m^3*
h	*Heat transfer coefficient, $(W/m^2 \cdot K)$*	Y	*Kinematic viscosity*, m^2/s
He	*Helical coil number*	E	*Heat exchanger effectiveness*
k	*Thermal conductivity*, *W/m·K*	ε'	*Modified effectiveness*
L_c	*Total length of coils*, m		**Subscript**
$LMTD$	*Logarithmic mean temperature difference, °C*	c	*Coil*
$m\dot{m}$	*Mass flow rate*	i	*Inner*
m_r	*Tube-side to shell-side mass flow rate ratio, ($\dot{m}_c / \dot{m}_{sh}$)*	o	*Outer*
N	*Number of coils turns*	r	*Ratio*

NTU	*Number of heat transfer units*	*Sh*	*Shell*
Nu	*Nusselt number*	*s*	*Surface*
P	*Coil pitch, mm*	*St*	*Straight tube*
Pr	*Prandtl number*	*t*	*Tube*
Q	mean velocity components, w		
Re	*Reynolds number*		
R^2	*Correlation Coefficient*		
T	*Temperature*		

INTRODUCTION

Helically coiled-tube heat exchangers are one of the most common equipment found in many industrial applications ranging from solar energy applications, nuclear power production, chemical and food industries, environmental engineering, and many other engineering applications. Helical coils are used for transferring heat in chemical reactors and agitated vessels because heat transfer coefficients are higher in helical coils. This is especially important when chemical reactions have high heats of reaction are carried out and the heat generated (or consumed) has to be transferred rapidly to maintain the temperature of the reaction. Also, because helical coils have a compact configuration, more heat transfer surface can be provided per unit of space than by the use of straight tubes. The centrifugal force enhances the heat transfer rate. This phenomenon can be beneficial especially in laminar flow regime. Comparison of heat transfer rates between a straight tube heat exchanger and a helically coiled heat exchanger were investigated by Prabhanjan et al. **[1].** They studied the relative advantage of using a helically coiled heat exchanger versus a straight tube heat exchanger for heating liquids. Most studies focus on constant wall temperature or constant heat flux, where as in this study it was a fluid-to-fluid heat exchanger. Results showed that the heat transfer coefficient was affected by the geometry of the heat exchanger and the temperature of the water bath surrounding the heat exchanger. All tests were performed in the transitional and turbulent regimes. Use of a helical coil heat exchanger was seen to increase the heat transfer coefficient compared to a similarly dimensioned straight tube heat exchanger. Temperature rise of the fluid was found to be effected by coil geometry and by the flow rate. Both heat exchangers had higher heat transfer coefficients when the bath temperature was increased. Thermal performance and pressure drop of a shell and helically coiled tube heat exchanger with and without helical crimped fins have been investigated by Naphon **[2]** .He used two different coil diameters with 9.5mm diameter copper tubes having

thirteen turns were used. Hot and cold water were used as working fluid in the range between 0.10 and 0.22kg/s and between 0.02 and 0.12kg/s, respectively. They have shown that with increasing hot water mass flow rate friction factor decreased. Rennie **[3]** studied the double-pipe helical heat exchangers numerically and experimentally neglecting the effect of coiled tube pitch. A double-pipe helical heat exchanger has been numerically modeled for fluid flow and heat transfer characteristics under different fluid flow rates and tube sizes. Dean Numbers for the inner tube ranged from 38 to 350. For all cases, the mass flow rates in the annulus were either half, equal, or double the flow rate in the inner tube. Two different tube diameter ratios were used. The overall heat transfer coefficients were calculated for both parallel flow and counter flow. The three-dimensional governing equations for momentum, continuity, and heat transfer were solved using a finite volume based computational fluid dynamics (CFD) code. Validation of simulations were conducted by comparing the Nusselt Numbers in the inner tube with those found in literature, the results fell within the range found in the literature. For the parameters tested in this study, the greatest thermal resistance was found in the annular region of the heat exchanger. The thermal resistance of this area could be decreased by increasing the inner tube diameter or by increasing the flow rate in the annulus. The Nusselt Number in the annulus was correlated with a modified Dean number as:

$$Nu = 0.075De + 5.36 \quad \ldots (1)$$

It shows a strong linear relationship for the considered range of Dean Numbers in this work.

The heat transfer coefficients of shell and helically coiled tube heat exchangers were investigated experimentally by Salimpour **[4]**. Three heat exchangers with different coil pitches were selected as test section for both parallel-flow and counter-flow configurations. All the required parameters like inlet and outlet temperatures of tube-side and shell-side fluids, flow rate of fluids, etc. From the results of this study, it was found that the shell-side heat transfer coefficients of the coils with larger pitches are higher than those for smaller pitches. Both numerical and experimental investigations were conducted to understand convective heat transfer from a single round pipe coiled in rectangular pattern by Conté and Peng **[5].** They studied heat exchangers are composed with inner and outer coils so that the exterior flow is very similar to flow within tube-bundles. The inner and outer coils of the heat exchangers are in turn composed of bends and straight portions. Calculations and experiments were done for two cases with different outside flow arrangements. The results showed the effects of geometric arrangement with better heat transfer for the case 1 of staggered arrangement mainly due to its more tortuous flow characteristics and better mixing of the exterior fluid. The numerical and experimental results qualitatively agree well with each other. The numerical and experimental results showed that coiling a pipe so that an exterior fluid flows over or in tube bundle can help to induce the turbulence without increasing the velocity. A numerical investigation of the forced convection heat transfer from vertical helically coiled tubes at various Reynolds and Rayleigh numbers, various

coil-to-tube diameter ratios and nondimensional coil pitches was studied by Mirgolbabaei et al. **[6]**. They found that with increasing dimensionless coil pitch in medium range, the heat transfer coefficient decreases while with increasing the pitch to 2 tube diameter, heat transfer coefficient is increased. Also it was concluded that heat transfer coefficient decreases by increasing the tube diameter for the same dimensionless coil pitch. They used different characteristic lengths in the Nusselt Number calculations to determine which length best fits the data and finally it has been shown that the normalized length of the shell-side of the heat exchanger reasonably demonstrates the desired location. Rahul et al. **[7]** has studied the Development of heat transfer coefficient correlation for concentric helical coil heat exchanger. In this study deals with developing a Correlation for heat transfer coefficient for flow between concentric helical coils. Existing Correlation is found to result in large discrepancies with the increase in gap between the concentric coils when compared with the experimental results. The results experimental data and CFD simulations using Fluent 6.3.26 are used to develop improved heat transfer coefficient correlation for the flue gas side of heat exchanger. Mathematical model is developed to analyze the data obtained from CFD and experimental results to account for the effects of different functional dependent variables such as gap between the concentric coil, tube diameter and coil diameter which affects the heat transfer. One extra parameter has been introduced to capture the strong correlations between coil gap and heat transfer coefficient. A wide range of data has been analyzed, which covers a wide range of the Reynolds number from 20 000 to 150 000. It is found that the extreme range of data identified by the ratio of coil gap and tube diameter can introduce significant error in the equation (2). The developed equation is only valid, if the specified ratio (Coil gap/ Tube diameter) is from 0.55 to 2.25. This covers the most of the practical range of the helical coil heat exchanger application.

$$Nu = 0.02652\,\mathrm{Re}^{0.83469}\,\mathrm{Pr}^{0.3}(Gap-ratio)^{-0.09685} \quad \ldots. (2)$$

An experimental investigation by Salimpour **[8]** was performed to study the heat transfer characteristics of temperature dependent-property using engine-oil inside shell and coiled tube heat exchangers. For this purpose, a well instrumented set-up was designed and constructed. Three heat exchangers with different coil pitches were tested for counter-flow configuration. Engine-oil was circulated inside the inner coiled tube, while coolant water flowed in the shell. They found that the increment of oil inlet temperature decreases the heat transfer coefficients. Also, the coil-side heat transfer coefficients of the coiled tubes with larger pitches are less than those of smaller pitches; and the effect of pitch on Nusselt number is more discernible in high temperatures. Finally, based on the results of this study, a correlation was developed to predict the coil-side heat transfer coefficients of the shell and coiled tube heat exchangers the following functional relationship is assumed:

$$Nu_i = 0.554 De^{0.496} \gamma^{-0.388} \Pr^{-0.151} \phi^{0.153} \quad \text{.....(3)}$$

where:
$\emptyset = \Pr_b / \Pr_w$ is the correction factor considered to take into account the effect of variable properties of the fluid.

$$\gamma = p / \pi D_c, \text{ b = oil and w = water}$$

The convective heat transfer coefficients in a spiral coil heat exchanger were investigated experimentally by Naphon and Wongwises **[9].**The test section is a spiral coil heat exchanger which consists of six layers of spiral coiled tubes. Each tube is fabricated by bending a 9.27 mm diameter straight copper tube into a spiral coil of five turns. The experiments are done under dehumidifying conditions. The results from the experiments are compared with those calculated from correlations in other studies. In addition, a new correlation for the tube side heat transfer coefficients for spirally coiled tube used under dehumidifying conditions is proposed for practical applications such as:

$$Nu_{ave} = 27.358 De^{0.287} \Pr^{-0.949} \quad \text{..... (4)}$$

For $De \geq 300, \Pr \geq 5$

Thermal performance of shell-and-coil heat exchangers were investigated experimentally by Nasser et al. **[10].** In this study an experimental investigation of the mixed convection heat transfer in a coil-in-shell heat exchanger is reported for various Reynolds and Rayleigh numbers, various tube-to-coil diameter ratios and dimensionless coil pitch. The purpose of this article is to assess the influence of the tube diameter, coil pitch, shell-side and tube-side mass flow rate over the performance coefficient and modified effectiveness of vertical helical coiled tube heat exchangers. The calculations have been performed for the steady-state and the experiments were conducted for both laminar and turbulent flow inside coil. It was found that the mass flow rate of tube-side to shell-side ratio was effective on the axial temperature profiles of heat exchanger. The results also indicate that the ε-NTU relation of the mixed convection heat exchangers was the same as that of a pure counter-flow heat exchanger.

Although there are many works in coil side of shell-and-coil heat exchanger correlated to heat transfer coefficient and natural convection on shell-side, but there are not many investigations on shell side and forced and mixed convection. In the present study the mixed convection heat transfer in a coil-in-shell heat exchanger for various Reynolds numbers, various tube-to-coil diameters ratio and different dimensionless coil pitch was experimentally investigated. The experiments were conducted for turbulent flow inside coil.

GEOMETRYOF SHELL AND COILED TUBE HEAT EXCHANGER

A typical shell and coiled tube heat exchanger is shown in Figure (1). In this figure, D_c is the diameter of the coil, $D_{sh,i}$ is the inner diameter of shell, $D_{sh,o}$ is the outer diameter and P is the coil pitch. The curvature ratio is defined as the coil-to-tube diameter ratio, d_t / D_c , and the non-dimensional pitch. The specification of heat exchanger is given in Table (1).

EXPERIMENTAL SET-UP

A schematic diagram of the experimental apparatus is shown in Figure (2) The test loop consists of a test section, hot water loop, cold water loop. The set up is a well instrumented single-phase heat exchanging system in which a hot water stream flowing inside the tube-side is cooled by a cold water stream flowing in the shell-side. The main parts of the cycle are coiled tube heat exchanger (1), measuring pot (2), storage tank (3), centrifugal pump (4), and heater (5). The heat exchangers include a copper coiled tube and an insulated shell. Water was used as the hot and cold fluid whereas hot water was pumped to the tank and coil, passing through gas heater. The flow rate for hot water was measured by using a calibrated measuring cylinder and a stopwatch positioned at the outlet of heat exchanger but for cold water by using the volumetric flow meter. The temperature of the inlet water of coiled tube to the heat exchanger was controlled by thermostat. Four constant temperatures (50, 60, 70 and 80 $^{\circ}$c) were considered for inlet mass flow rate of coil and water inlet temperature to the shell side was the temperature of the tap water. Temperatures were measured using eight K-type thermocouples placed at equally distanced locations in order to measure the coil surface and the fluid temperature. Four other thermocouples were located at inlets and outlets of heat exchanger to measure the temperatures of the hot and cold. Figure (3) shows the apparatus arranged for heat exchanger experiments. The coil was formed carefully by using 9.47 and 12.59 mm OD straight copper tubing, located the middle of the circular space of the shells of heat exchanger. The range of experimental conditions in this study is given in Table (2).

DATA COLLECTION AND ANALYSIS

For determining the heat flux rate, assumed that the thermal resistance of the copper tube wall was negligible [10]. A temperature of coil surfaces was taken as equal to the water temperature inside the coil at the same location in order to calculate local heat flux. An overall energy balance was performed to estimate the extent of any heat losses or gains from the surrounding.

According to the research of Srinivasan [11], the critical Reynolds number for the helical pipe flow, which determines the flow is laminar or turbulent, is related to the curvature ratio as follows:

$$Re_{crit} = 2100\,[1+ 12(d_{in}/ D_c)^{0.5}] \quad \ldots. (5)$$

$$Q_c = m_c cp_c \left(T_{c_i} - T_{c_o}\right) \quad \ldots (6)$$

$$Q_{sh} = m_{sh} cp_{sh} \left(T_{sh_o} - T_{sh_{in}} \right) \quad \text{....(7)}$$

$$Q_{avg} = \frac{Q_c + Q_{sh}}{2} \quad \text{..... (8)}$$

In the present study, only the data that satisfy the energy balance conditions; $[Q_c - Q_{sh}] / Q_{avr}$ is less than 10%, are used in the analysis. Experiments were conducted with various inlet temperatures and flow rates of hot water and cold water entering the test section.

$$\frac{1}{U} = \frac{1}{h_i} + \frac{1}{h_o} \quad \text{..... (9)}$$

$$h_i = \frac{Q_{(avg)}}{A_i (T_{c_w} - T_{cs})} \quad \text{..... (10)}$$

$$h_o = \left[\frac{1}{U} - \frac{1}{h_i} \right]^{-1} \quad \text{..... (11)}$$

$$Nu_c = \frac{h_i D_{t_i}}{k} \quad \text{..... (12)}$$

$$Nu_{sh} = \frac{h_o D_h}{k} \quad \text{..... (13)}$$

ERROR ANALYSIS

As with report of every experimental research, the analysis of the experimental uncertainties in calculating the results must be given proper attention. The method proposed by Kline and McClintock [12]. The results are shown in Eq. (14).

$$Nu_{exact} = Nu_{experiment} \pm (0.023032 - 7.889717) \quad \text{.... (14)}$$

RESULTS AND DISCUSSION

Results of the Effect of the ratio of mass flow rate of coil-side to shell-side ratio (m_r) on the axial temperature profiles of heat exchanger for counter-flow are shown in Figures (4**)** to **(9)**. The profiles in counter flow tend to be concave up,

which means that the coil surface temperature is higher than usual at the top and then it drops faster than usual while moving toward the bottom of the heat exchanger. Figures (4), (5) show typical temperature distributions for coil#1 and coil#2 inside the heat exchanger for fixed inlet conditions (m_r=0.24 and $T_{c,i}$=80°C). The nonlinearity coil temperature distribution is such that the profiles tend to be concave up, which means that the coil surface temperature is higher than usual at the top and then it drops faster than usual while moving towards the bottom of the heat exchanger.

Figures (6), (7) show typical temperature distributions for coil#1 and coil#2 inside the heat exchanger for fixed inlet conditions (m_r=1 and $T_{c,i}$ =80°C). The temperature rise of a cold fluid is equal to the temperature drop of the hot fluid is when the heat capacity rates of the two fluids are equal to each other ($C_c \approx C_{Sh}$), that means axial temperature profile of the coil surface is close to from being linear for those figures.

Figures (8), (9**)** show typical temperature distributions for coil#1 and coil#2 inside the heat exchanger for fixed inlet conditions(m_r=4 and $T_{c,i}$ =80°C). The axial temperature profile of the shell-side water is far from being linear for those figures.

It can be seen that as the mass flow rate ratio changes, the temperature profile changes from an initially concave-up profile to concave-down one. In other words the coil surface is colder than usual at the top part and its temperature gradually decreases until it reaches its lowest value at the bottom of heat exchanger. The value of m_r=1 seems to be the critical point. For m_r significantly less than unity the curves deviate greatly from being linear whereas the curves are close to a straight line for $m_r \approx 1$. The linear temperature profile means that the shell-side heat transfer coefficient is constant along the axis of the heat exchanger. There is a notable drop in coil surface temperature. The curves suggest that the shell-side heat transfer coefficient is no longer constant. Since it is reasonable to assume that the heat transfer is uniform, the product ($h_o \Delta T$) is constant along the coil surface. Therefore a smaller temperature difference means a higher h_o value. The magnitude of h_o starts from a low value at the top and gradually increases to its highest value at the bottom of the heat exchanger. Obviously this situation is not desirable since the hot stream forfeits its heat very quickly and therefore the heat exchanger does not operate at its full capacity. It can be concluded that for such a low shell-side mass flow rate, the heat exchanger is oversized in terms of the surface area.

Figure (10**)** shows typical relationship between the inlet coil temperature with the *LMTD* for fixed inlet conditions (m_r=1.5) and different coil pitches. It is obvious that the *LMTD* increases with increase inlet hot water temperature due to the increase in the temperature difference between the cold water temperature and surface coiled tube temperature. It can be seen that for a fixed value of m_r, the effect of the increase in the inlet coil temperature on *LMTD* is positive effect. Physically, increasing the inlet coil temperature leads to an increase in the heat extracted from the hot stream which translates into an increases in the value of the *LMTD.*

Figure (11) reveals the relation between the heat transfer rates with mass flow rate ratio for different coils and for both parallel-flow and counter-flow configurations. The heat transfer rates are highly dependent on decreasing the

thermal resistance of the coiled tube. Physically, increasing the inlet coil mass flow rate leads to a decreasing in the thermal resistance which translates into an increases in the value of the heat lode. These figure show that the heat load of the coil#2 is higher than the heat load of the coil#1 and coil#3 due to increase of the surface area of the coil#2. The advantage in using the heat transfer in the counter flow configuration and the parallel flow configuration is shown in same figure. The graph shows the increase in the heat transfer expected when the flow is changed from parallel flow to counter flow. Also a heat transfer rate of the counter flow is higher than parallel flow due to increase of the LMTD.

In Figures (12) and (13), the modified effectiveness as defined by Eq. (15) **[10]** are plotted as a function of the mass flow rate ratio for both parallel-flow and counter-flow configurations. Modified effectiveness is a ratio between the actual temperature drops in coil to maximum possible temperature drops in coil. Results of the effect of the mass flow rate on the modified effectiveness of the counter flow are shown in Figure (12), this figure shows the results of present work and Ref. [10].

$$'\varepsilon = \frac{T_{ci} - T_{co}}{T_{ci} - T_{shi}} \qquad \text{……. (15)}$$

Two results show a good agreement between the two works with an error ratio of 2.026%. The modified effectiveness decreases rapidly when mass flow rate ratio increases from (0.24 – 2) for counter and parallel flow, while for values larger than 2 the modified effectiveness remains nearly unchanged. This means that for a certain heat exchanger, increment of tube-side mass flow rate will always downgrade the effectiveness. The data can be correlated by a simple power equation. Eq. (16) is recommended for predicting the effectiveness of heat exchanger in the range of $\mathbf{m_r}$ from (0.25 to 4).

$$'\varepsilon = 0.4841(m_r)^{-0.4724} = 0.4841\left(\frac{m_{sh}}{m_c}\right)^{0.4724} \qquad \text{…... (16)}$$

This equation indicates that modified effectiveness is a strong function of the mass flow rate ratios. The shell-side water mass flow rate has a favorable effect and tube-side mass flow rate has an adverse effect on the modified effectiveness of the heat exchanger. Physically, increasing the mass flow rate ratio means more coil-side mass flow rate leads to less temperature fall in the hot stream and consequently worsen the modified effectiveness of the heat exchanger. On the contrary, little coil- side mass flow rate leads to more temperature fall in the hot stream and consequently better the modified effectiveness of the heat exchanger. The two mass flow rates, therefore act against each other with the same strength. Using the definition of the modified effectiveness Eq. (15) and Eq. (16), one can easily derive equations for predicting the tube-side outlet temperature.

$$T_{co} = T_{ci} - 0.48411 \left(\frac{m_{sh}}{m_c} \right)^{0.4724} * (T_{ci} - T_{shi}) \qquad \ldots\ldots\ (17)$$

In general, the inlet temperatures are known, the outlet temperatures of coil side can be predicted.

Figure (13) shows the results of the effect of the mass flow rate on the modified effectiveness of the parallel flow as follow:

$$'\varepsilon = 0.4172(m_r)^{-0.4839} = 0.4172 \left(\frac{m_{sh}}{m_c} \right)^{0.4839} \qquad \ldots..(18)$$

$$T_{co} = T_{ci} - 0.4172 \left(\frac{m_{sh}}{m_c} \right)^{0.4839} * (T_{ci} - T_{shi}) \qquad \ldots\ldots\ (19)$$

The *U.A* product, of the heat exchanger indicates the ability to transfer heat between the hot and cold streams at a certain mean temperature difference. The rate of heat transfer increases with increasing the overall heat transfer coefficient multiplied by surface area to coil of the heat exchanger, because heat transfer rate increase as a result of both shell-side and tube-side heat transfer coefficient increase. This is evident from Figures (14) and (15) which include the data from all tests for both counter flow and parallel flow respectively. The *UA* product is plotted against the heat transfer rate multiplied by surface area to coil the effect of the surface area on the *UA* product. Physically, increasing the surface area increases the heat extracted from the hot stream which translates into an increase in the values of the overall heat transfer coefficient.

The results from the counter flow configuration were similar to the parallel flow, as is, as expected changing the flow direction should have negligible effects on the heat transfer coefficients. Heat transfer rates, however, are much higher in the counter flow configuration, due the increased log mean temperature difference. The counter flow versus the parallel flow overall heat transfer coefficients are plotted in Figure (16), where the values plotted against each other are from the same experimental parameters. There is a reasonable agreement between the two values.

Figure (17) shows the overall heat transfer coefficients versus the Dean number for the counter flow. The overall heat transfer coefficients increase with increasing inner Dean Number. However, the significance of the increase is a function of the ratio of the mass flow rates. The mass flow rate ratio has a significant effect on the overall heat transfer coefficient, raising the overall heat transfer coefficient when the flow rate in the coil-side is increased.

Figures (18) and **(**19) depict the variation of the effectiveness for the coiled tube with the number of transfer units (*NTU*) at (C_r) in the range of (0.24 to 0.99) for both the counter flow and the parallel flow configurations**.** On these Figures the

theoretical curves are plotted for capacity ratios of (C r=0) and (Cr=1). As can be seen, the simulation data fits well with these curves. These figures show that increasing the (*NTU*) for a specified (Cr) caused an increase in the effectiveness values. This is due to the dependence of the (*NTU*) and the effectiveness on the overall heat transfer coefficient, therefore, the increasing of the (*NTU*) means that the overall heat transfer coefficient increased at the given surface area, and this led to increase the effectiveness.

The shell-side heat transfer coefficient data was plotted versus heat flux for different coil pitch in Figure (20).As the figure shows, the heat transfer coefficient enhances with increasing the dimensionless coil pitch. From this figure, it appears that the increase of coiled tube pitch leads to higher values of shell-side heat transfer coefficient. This may be explained as in smaller coil pitches, the coolant water is confined in the space between the successive coil rounds and a semi-dead zone is formed. As in this region, the flow of shell-side fluid is decelerated; heat transfer coefficients will be descended. Also, it can be easily seen that the difference among the coils with different geometries are sprier in high heat flux region.

The recommended correlation for Nusselt number in turbulent flow in a straight tube is [13]:

$$Nu_{st} = 0.023\, Re^{0.8}\, Pr^{n} \qquad \ldots\ldots (20)$$

where: st refers to straight tube.

In which the Prandtl number index (n) is equal to (0.3) for the cooling process, and this equation is valid for turbulent flow and ($0.6 < Pr < 100$). Figure (21) shows the enhanced Nusselt number for different coil pitch. The increase in the coiled tube Nusselt number due to the secondary flow would take hotter fluid and pass it through the center of the tube. This would result in a faster transfer of heat from the tube surface to the center of the tube. The use of a helical coil heat exchanger was seen to increase the heat transfer coefficient compared to a similarly dimensioned straight tube heat exchanger. It could deduce from this figure that the enhancement in Nusselt number is well-defined in the turbulent flow.

NUSSELT NUMBER CORRELATIONS

Figure (22) plots the Nusselt and Prandtl numbers data based on the experimental results against the Dean number for coil#1 and ($R^2 = 0.903$) for this graph. The correlation of the current experimental data obtained from the curve fitting for the range of ($1 < m_r < 2$), ($4585 < De < 12117$) is as follow:

$$Nu_c = 0.13877 De^{0.7721} P_r^{0.3} \qquad \ldots\ldots (21)$$

where:

$$De = \mathrm{Re}\sqrt{\frac{D_t}{D_c}}$$

For coil#2 the correlation of the current experiment data obtained from the curve fitting in Figure (23), (R^2 = 0.97) for this graph and the range of ($1 < m_r < 2$), (3803< De < 9925) is as follow:

$$Nu_c = 0.02145 De^{0.9683} P_r^{0.3} \qquad \ldots\ldots. \quad (22)$$

And for coil#3 the correlation of the current experiment data obtained from the curve fitting in Figure (24), (R^2 = 0.91) for this graph and the range of ($1 < m_r < 2$), (3849< De < 10093) is as follow:

$$Nu_c = 0.0499 De^{0.91535} P_r^{0.3} \qquad \ldots\ldots (23)$$

Figure (25) plots the Nusselt and Prandtl numbers data based on the experimental results against the Helical coil number for different coil pitches and (R^2 = 0.903) for this graph. The correlation of the current experiment data obtained from the curve fitting for the range of ($1 < m_r < 2$), (3838< *He* < 12107) is as follow:

$$Nu_c = 0.0288 He^{0.9413} P_r^{0.3} \qquad \ldots.(24)$$

where:

$$He = De[1 + (P/\pi D_c)^2]^{-0.5}$$

Using the definitions of the He and De Eq. (25) can be easily derived.

$$Nu_c = 0.0288 \left[\frac{(D_t / D_c)}{1 + (P/\pi D_c)^2} \right]^{0.47065} \mathrm{Re}^{0.9413} \mathrm{Pr}^{0.3} \qquad \ldots..(25)$$

Correlation was developed to predict the shell-side Nusselt number based on the experimental results, a correlation between the Nusselt and Prandtl numbers versus Reynolds number for different coil pitches and (R^2 = 0.83) for this graph is presented in Figure (26). Also the correlation of the current experiment data obtained from the curve fitting for the range of ($1 < m_r < 2$), (1450< Re < 1807) is as follow:

$$Nu_{sh} = 0.0835 \mathrm{Re}^{0.9} P_r^{0.4} \qquad \ldots (26)$$

CONCLUSIONS

In this study, an experimental investigation into the convection heat transfer in a vertical helically coiled tube heat exchanger was carried out. The study has the following conclusions:

- The major effect on the axial temperature profiles of heat exchanger was the mass flow rate ratio (m_r)
- The modified effectiveness decreased with increasing mass flow rate ratio.
- The heat load of the coil#2 is higher than the heat load of the coil#1 and coil#3.
- The tube diameter was found to have negligible influence on the shell-side heat transfer coefficient but the coil pitch was found to have main influence
- The convection heat transfer coefficient of shell-side increases when the coil pitch increases.
- The heat transfer rate of heat exchanger increases as the overall heat transfer coefficient increases.

REFERENCES

[1].Prabhanjan,D. G. G. S. V. Raghavan and T. J. Rennie, Comparison of heat transfer rates between a straight tube heat exchanger and a helically coiled heat exchanger, lnt. Comm. Heat & Mass Transfer & Vol. 29. No. 2. pp. 185-191, 2002.

[2]. Naphon,P. Thermal performance and pressure drop of the helical-coil heat exchangers with and without helically crimped fins, International Communications in Heat and Mass Transfer 34 (3) (2007) 321–330.

[3]. Rennie, T.J. Numerical and experimental studies of a double-pipe helical heat exchanger, Ph.D. Thesis, McGill University, Montreal, Canada, 2004.

[4]. Salimpour ,M.R. Heat transfer coefficients of shell and coiled tube heat exchangers , Experimental Thermal and Fluid Science 33 (2009) 203–207

[5]. Conté,I. X.F. Peng , Numerical and experimental investigations of heat transfer performance of rectangular coil heat exchangers , Applied Thermal Engineering 29 (2009) 1799–1808

[6]. Mirgolbabaei,H. H. Taherian, G. Domairry, N. Ghorbani, Numerical estimation of mixed convection heat transfer in vertical helically coiled tube heat exchangers, International Journal for Numerical Methods in Fluids, in press.

[7].Rahul Kharat, Nitin Bhardwaj*, R.S. Jha , Development of heat transfer coefficient correlation for concentric helical coil heat exchanger , International Journal of Thermal Sciences 48 (2009) 2300–2308

[8]. Salimpour,M.R. Heat transfer characteristics of a temperature-dependent-property fluid in shell and coiled tube heat exchangers, International Communications in Heat and Mass Transfer 35 (2008) 1190–1195

[9].Paisarn Naphon and Somchai Wongwises, An experimental study on the in-tube convective heat transfer coefficients in a spiral coil heat exchanger, Int. comm. Heat mass transfer,Vol.29, No.6, pp. 797-809, 2002

[10].Nasser Ghorbani, Hessam Taherian, Mofid Gorji and Hessam Mirgolbabaei, An experimental study of thermal performance of shell-and-coil heat exchangers, International Communications in Heat and Mass Transfer 37 (2010) 775–781.

[11]. Srinivasan, P.S. S.S. Nandapurkar, F.A. Holand, Friction factors for coils، Institution of Chemical Engineering Transaction 48 (1970) T156–T161.

[12]. Kline,S.J. F.A. McClintock, Describing uncertainties in single-sample experiments, Mechanical Engineering 75 (1953) 3–9.
[13]. Holman - Heat Transfer, P. McGraw Hill Publication, 9th Ed,(2002).

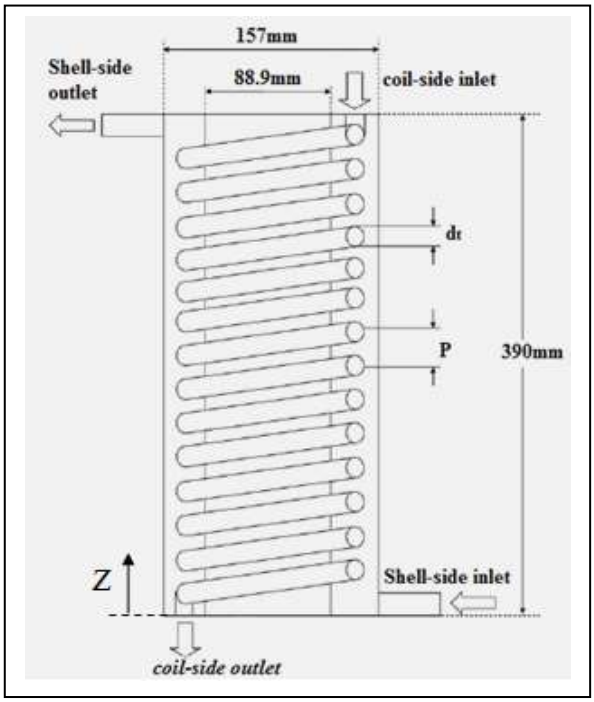

Figure (1) schematic diagram of a shell-and-coil

Table (1) Geometrical characteristics of the heat exchanger.

Item	*coil#1*	*coil#2*	*coil#3*
Coil diameter, tube-center-to-tube-center (D_c),(mm	125.7	128.3	128.3
Outside diameter of copper tube d_o, (mm)	9.47	12.59	12.59
Inside diameter of copper tube d_i, (mm)	7.77	10.82	10.82
Approximate number of turns in helical coil, N	24.8	24.9	14.42
Curvature ratio, d_t/D_c	0.0618	0.0843	0.0843
Axial length of helical coil L_c,(m)	9.8	10	5.86
Coil pitch, tube-center-to-tube-center P, (mm)	16.5	16.5	30.4
Heat exchanger height H, (mm)	390	390	390
Total surface area of the coil A,(m^2)	0.2915	0.3955	٢٣٥.
Nondimensional coil pitches $=p/\pi D_c$	0.0418	0.409	0.075

Table (2) the range of operating parameter

Parameter	Tube-side water flow rate	Tube inlet temperature	Tube outlet temperature	Shell inlet temperature	Shell outlet temperature
Range	(0.027- 0.11) kg/s	(50-80)°C	(27-70)°C	(19-24)°C	(29-75)°C

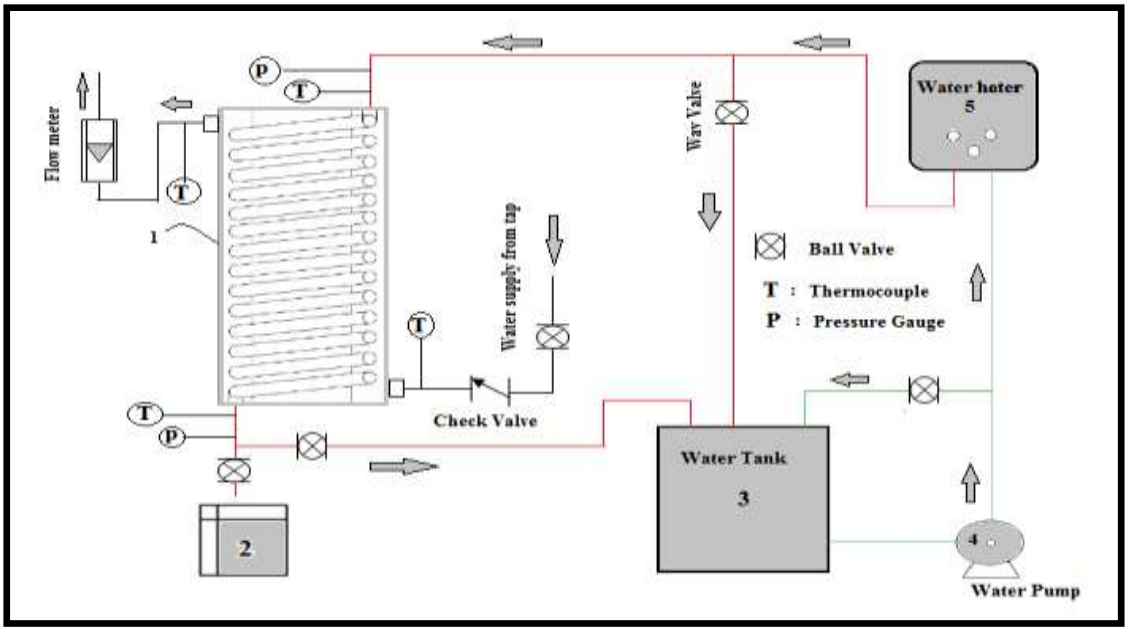

Figure (2) Flow diagram of the experimental set-up.

Figure (3) Apparatus for heat exchanger experiments.

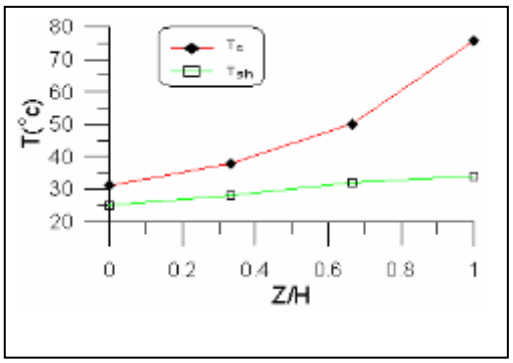

Figure (4) Temperature distribution along heat exchanger for coil#1 for m_r=0.24 (counter flow).

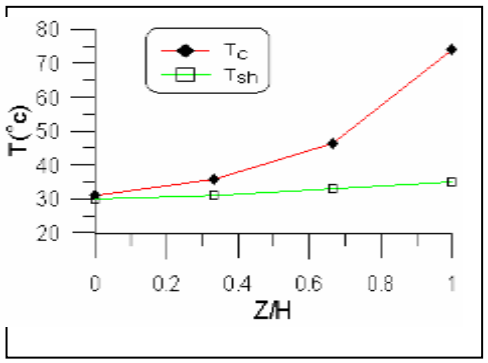

Figure (5) Temperature distribution along heat exchanger for coil#2 for m_r=0.24(counter flow).

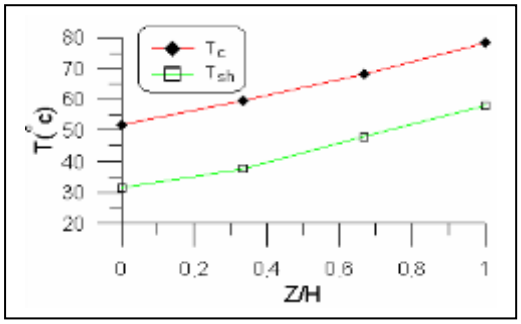

Figure (6) Temperature distribution along heat exchanger for coil#1 for m_r=1 (counter flow).

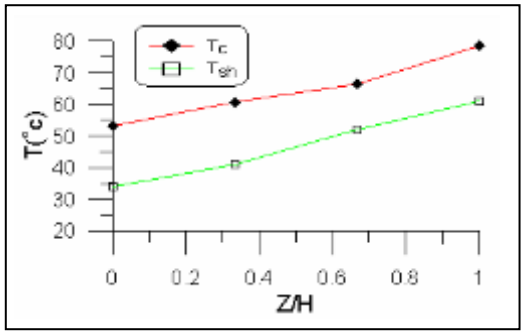

Figure (7) Temperature distribution along heat exchanger for coil#2 for m_r=1 (counter flow).

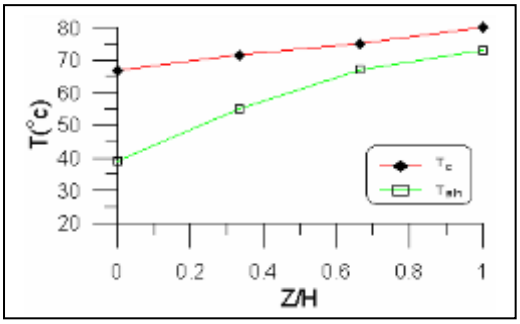

Figur (8) Temperature distribution along heat exchanger for coil#1 for m_r=4 (counter flow).

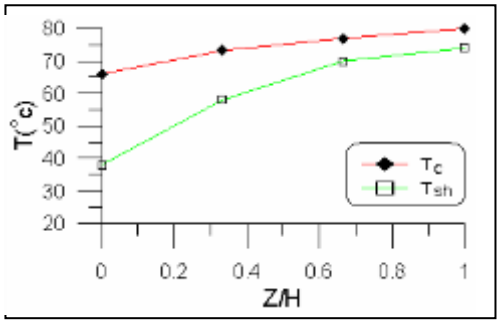

Figur (9) Temperature distribution along heat exchangerfor coil#2 for m_r=4 (counter flow).

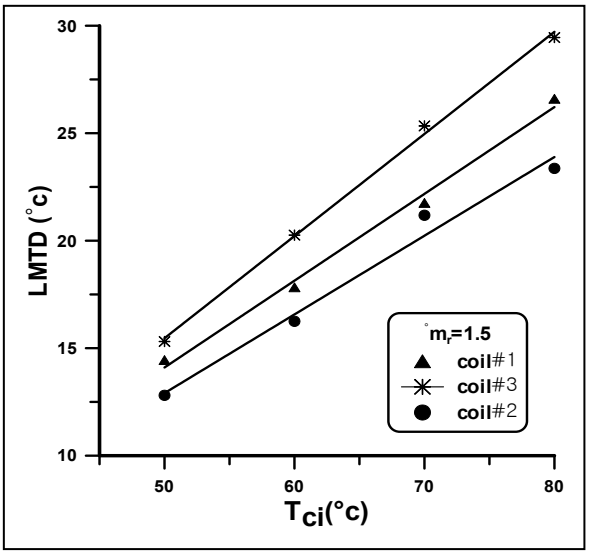

Figure (10) LMTD versus temperature coil-in (counter flow).

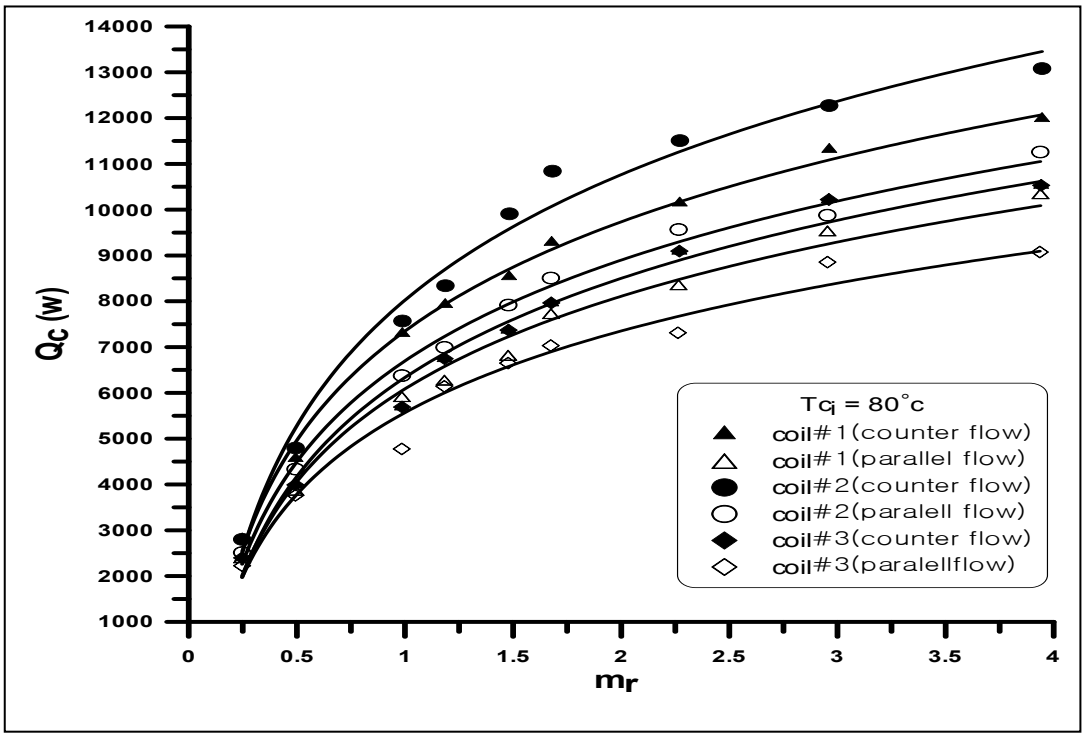

Figure (11) Heat transfer rate in the heat exchanger versus the mass flow rate ratio.

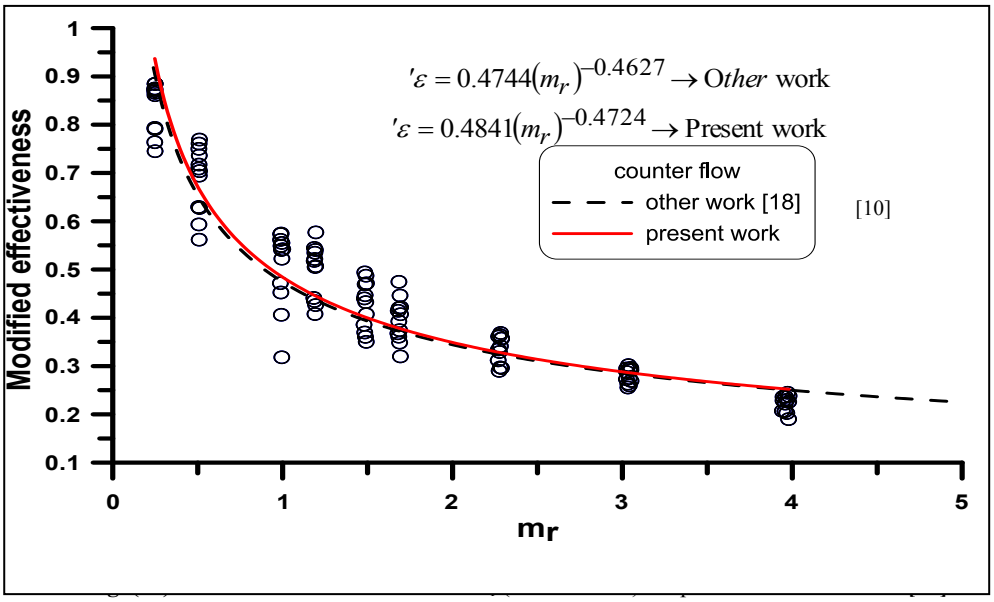

Figure (12) Modified effectiveness versus m_r (counter flow) for present and other work[10].

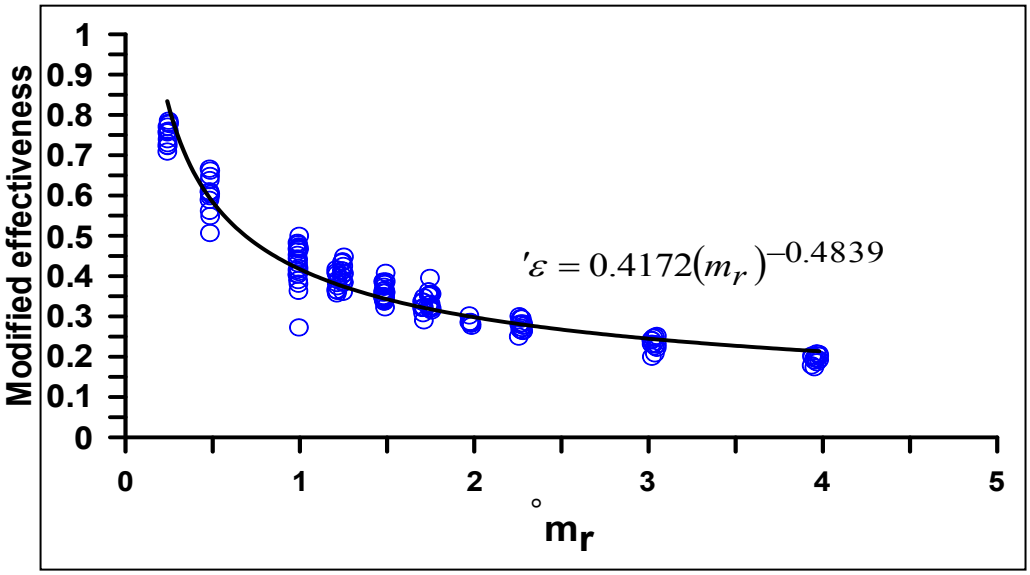

Figure (13) Modified effectiveness versus m_r for all test configurations (parallel flow).

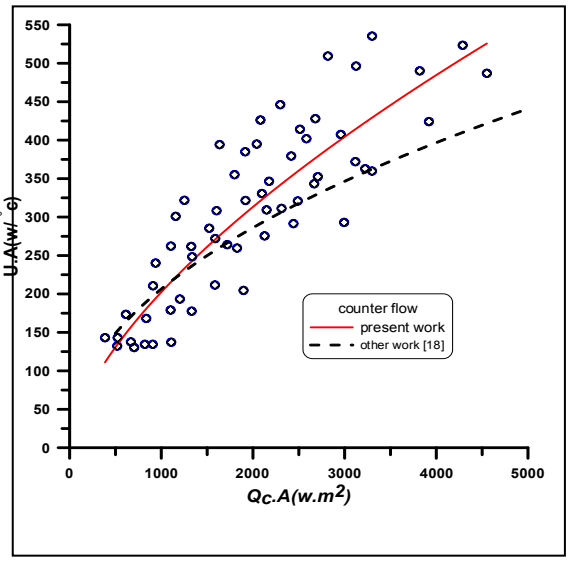

Figure (14) Variation of the overall heat transfer coefficient versus heat rate (Counter flow) for present and other work [10].

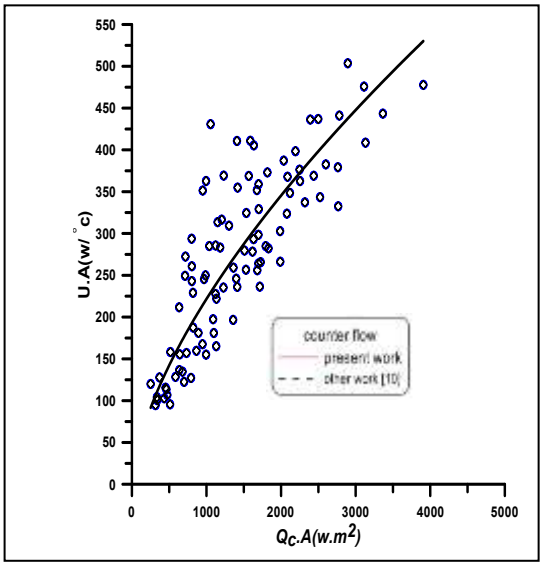

Figure (15) Variation of the overall heat transfer coefficient versus the heat rate (parallel flow).

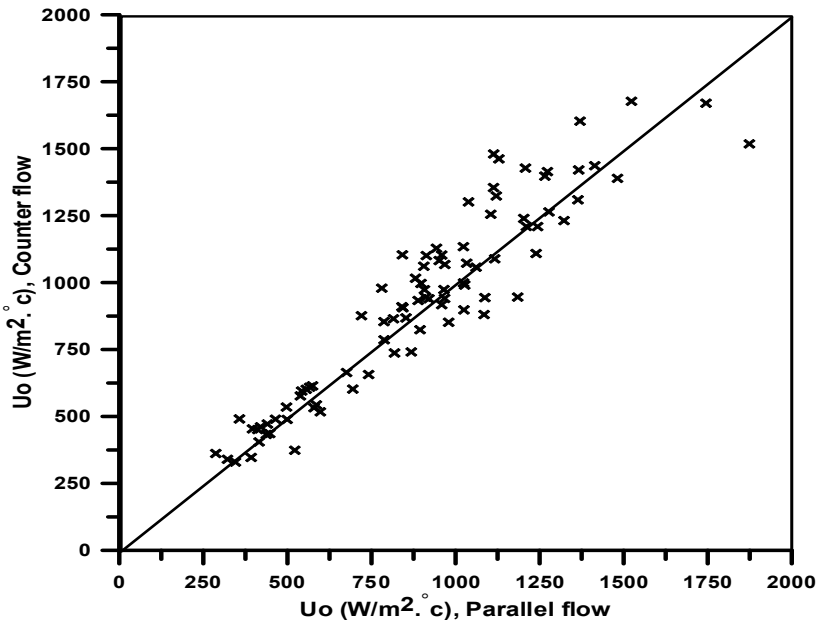

Figure (16): Counter flow overall heat transfer coefficient versus parallel flow overall heat transfer coefficient for all tests.

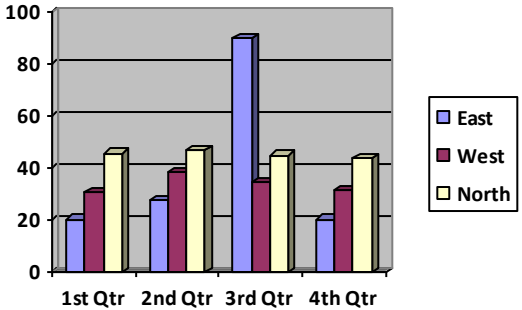

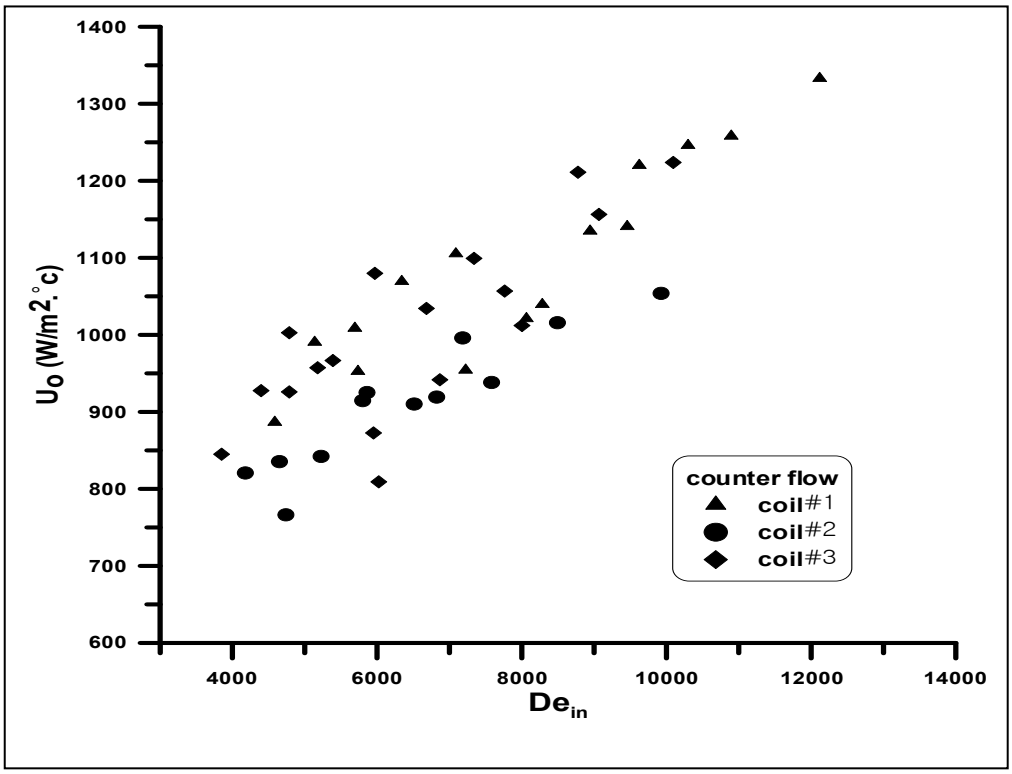

Figure (17): Overall heat transfer coefficient versus the Dean number.

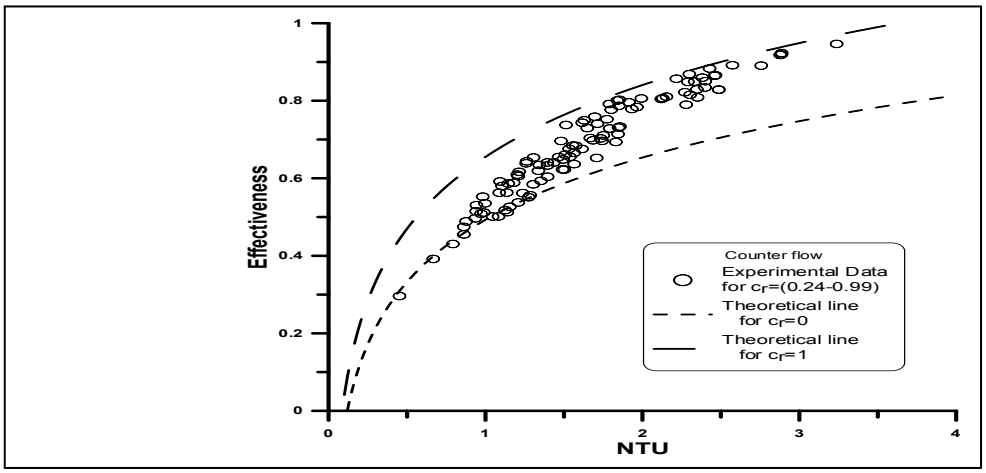

Figure (18) Effectiveness-NTU graph for counter flow in the helical coiled tube heat exchanger.

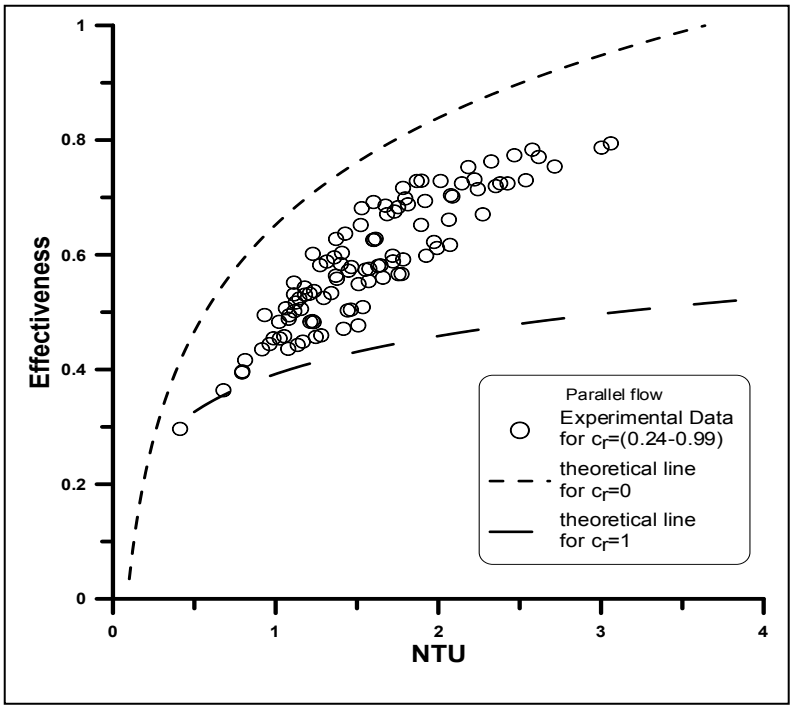

Figure (19) Effectiveness-NTU graph for parallel flow in the helical coiled tube heat exchanger.

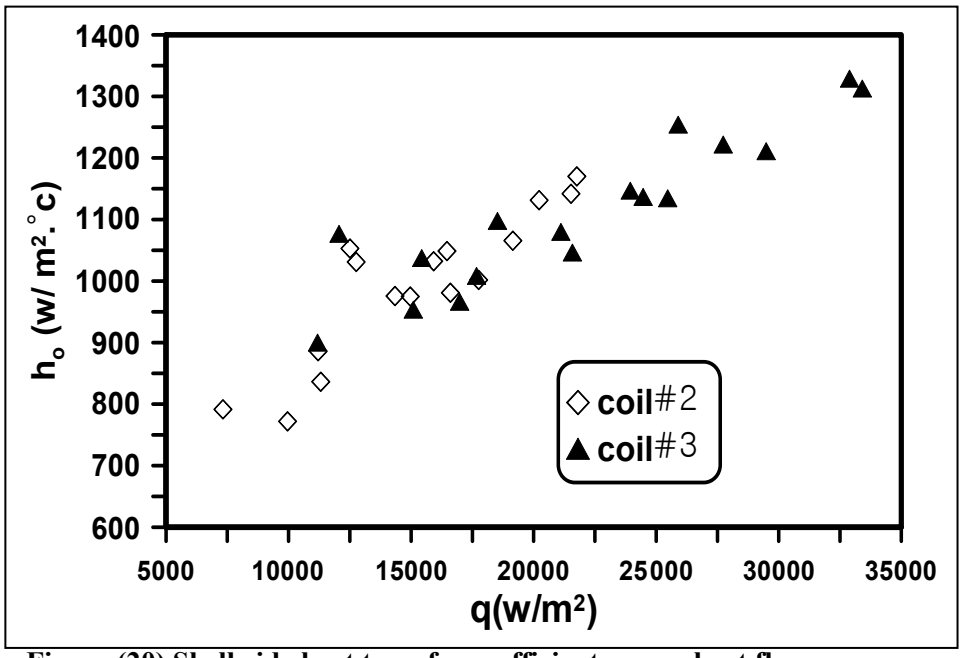

Figure (20) Shell-side heat transfer coefficient versus heat flux for various coil pitch.

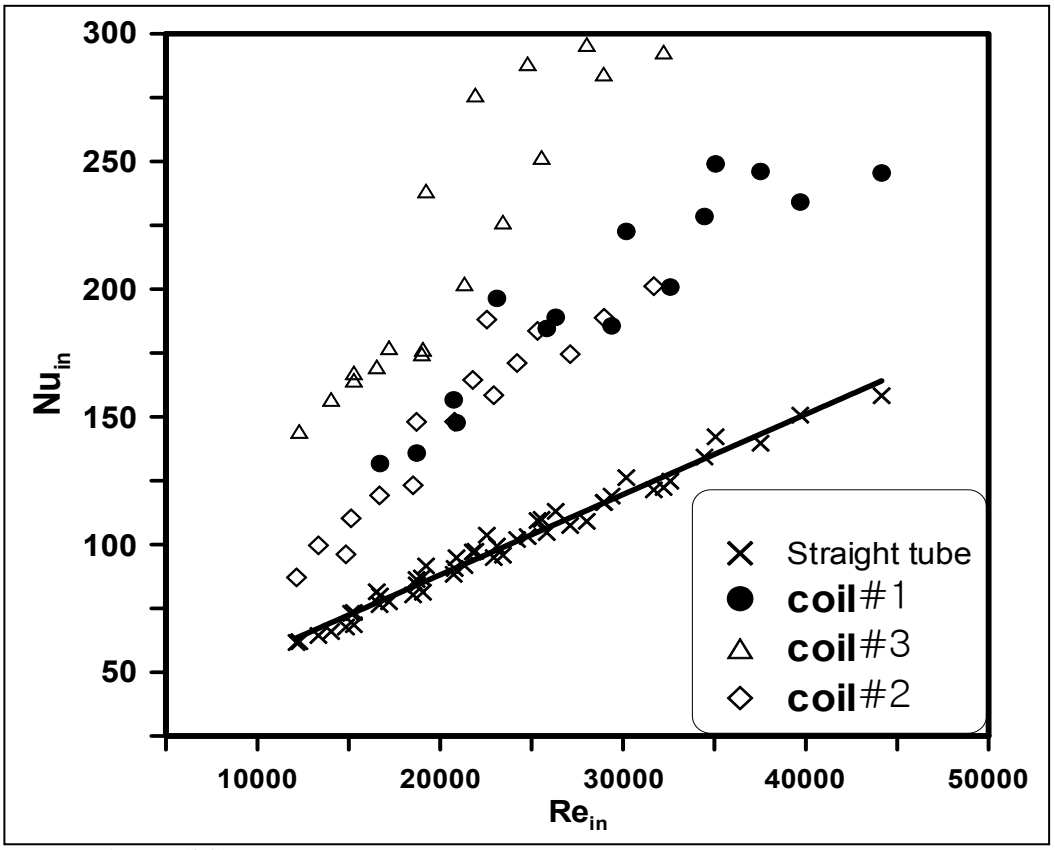

Figure (21) The Nusselt number versus the Reynolds number based on tube diameter for straight and coiled tubes.

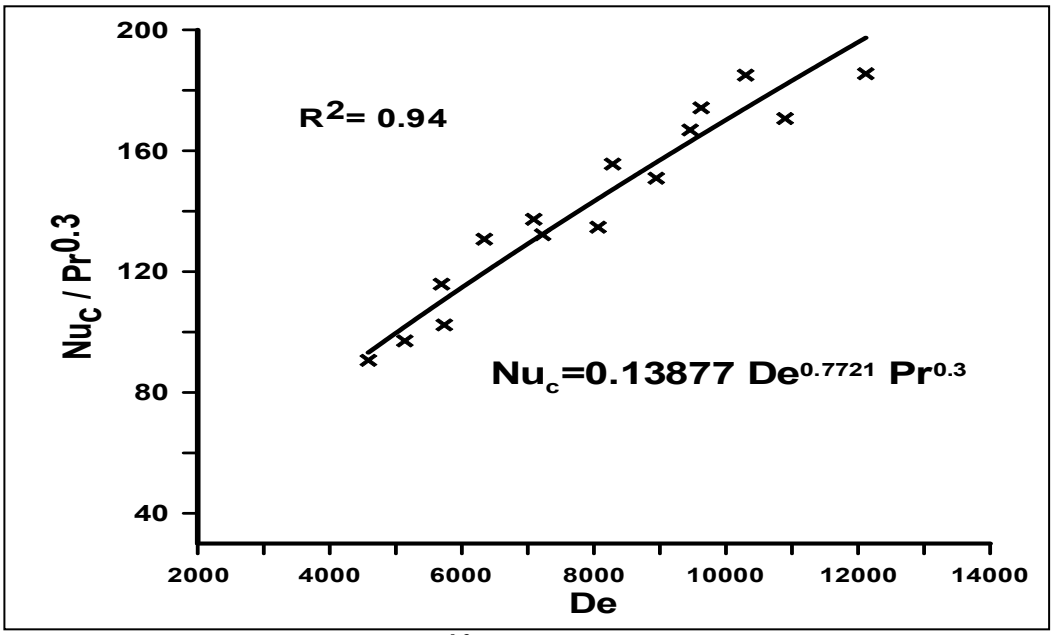

Figure (22) $Nu_c / Pr^{0.3}$ versus the Dean number for coil#1.

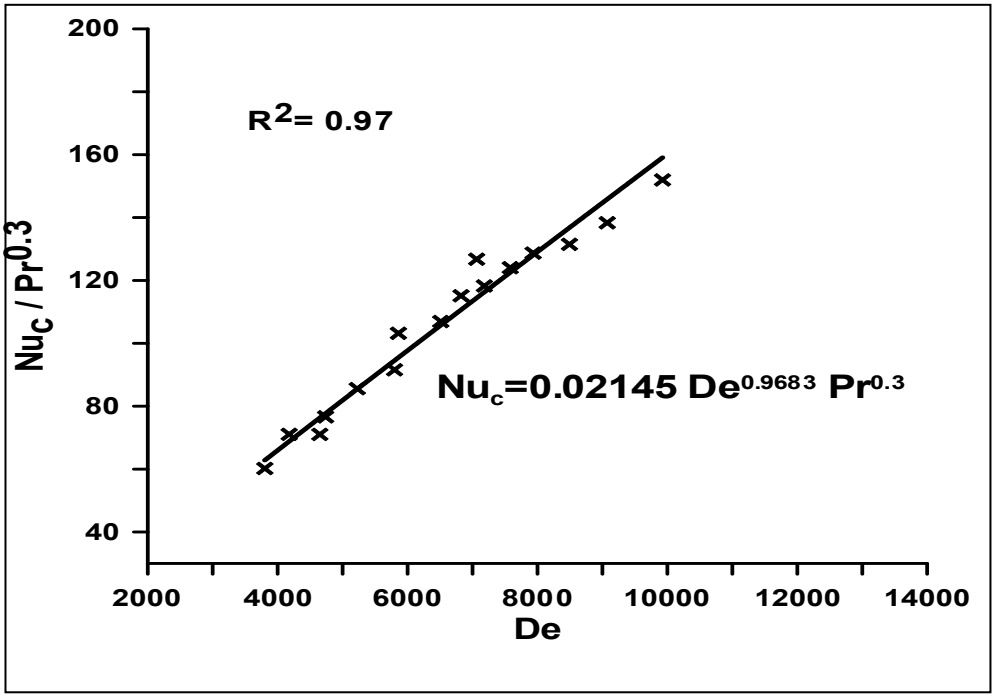

Figure (23) $Nu_c / Pr^{0.3}$ versus the Dean number for coil#2.

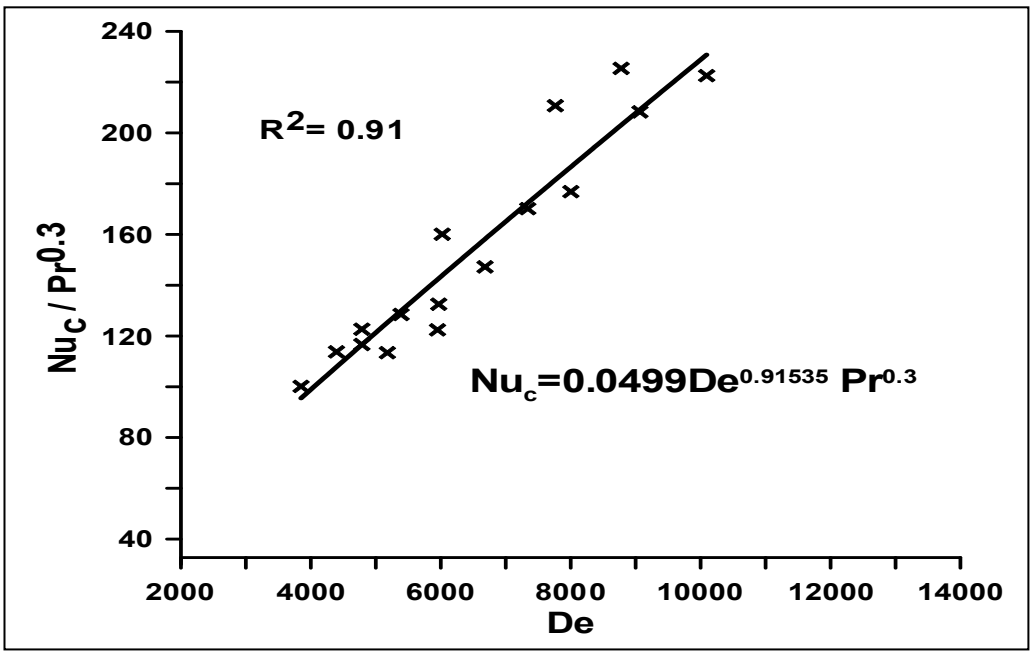

Figure (24) $Nu_c / Pr^{0.3}$ versus the Dean number for coil#3.

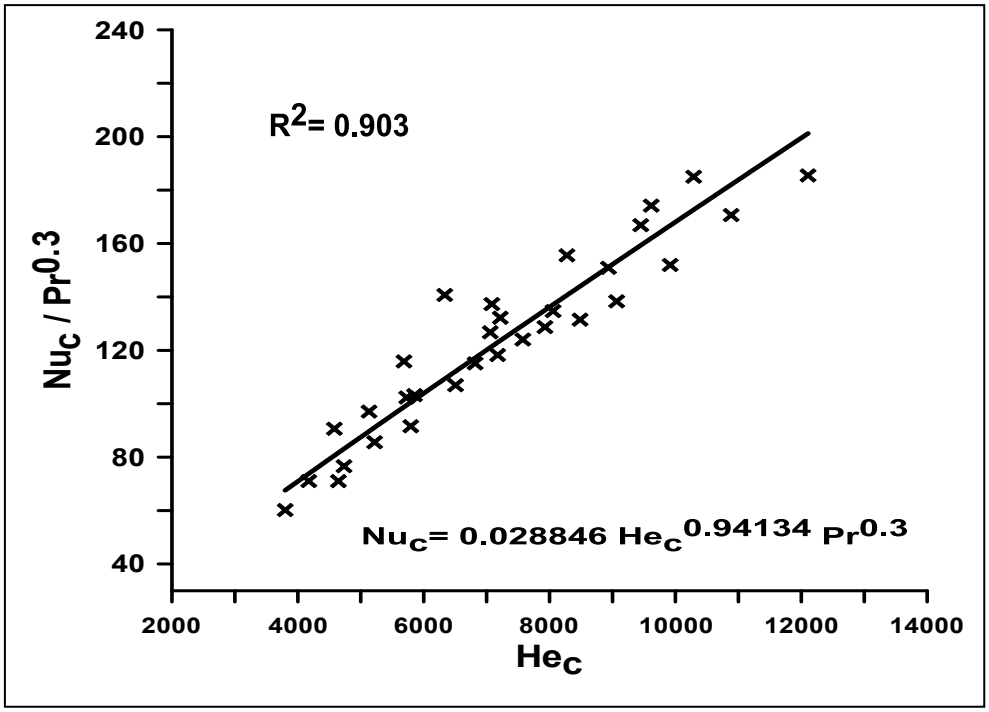

Figure (25) $Nu_c / Pr^{0.3}$ versus the helical coil number.

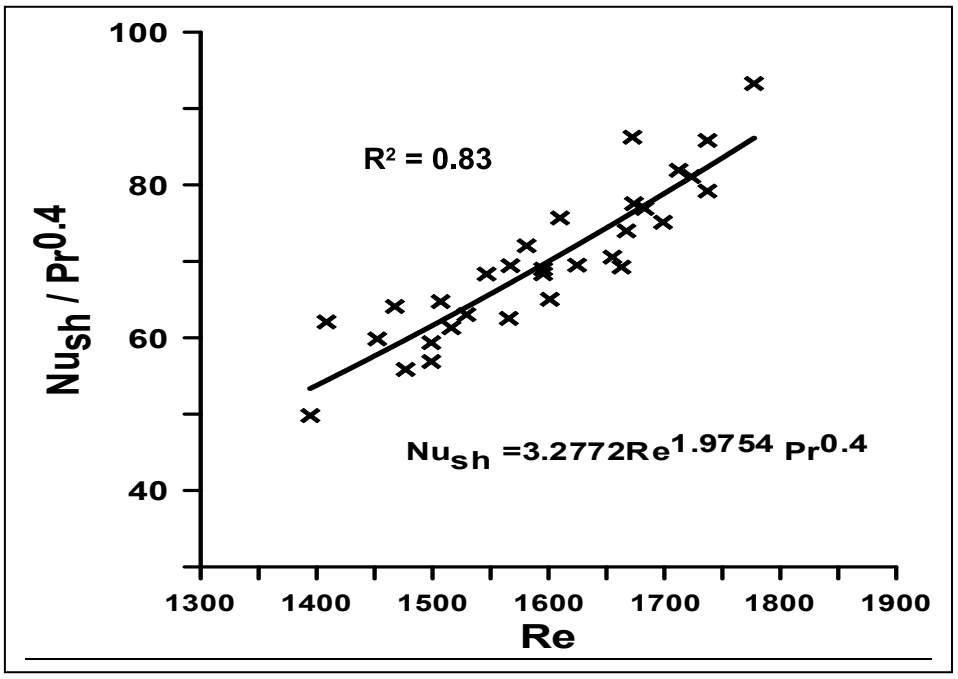

Figure (26) $Nu_{sh} / Pr^{0.4}$ versus the Reynolds number based on hydraulic diameter.